Gojko Magazinović

ISSN 0007-215X
eISSN 1845-5859

LEAST INERTIA APPROACH TO LOW-SPEED MARINE DIESEL PROPULSION SHAFTING OPTIMUM DESIGN

UDC 629.5.03
Original scientific paper

Summary

In this study, a novel approach to the low-speed marine diesel propulsion shafting design is proposed and examined. The proposed approach is based on the shafting least inertia principle, in which the design task is formulated and solved as a constrained nonlinear optimization problem. The core of the approach is a cost function, which is defined as a weighted sum of the shafting, turning wheel, and tuning wheel inertias, because it is a suitable proxy of the propulsion shafting material and production costs. The constraint set is composed of the three mandatory constraints, where the crankshaft, intermediate shaft, and propeller shaft torsional vibration stresses should be lower than the corresponding stress limits, as well as a few additional constraints that help ensure that the plant behavior complies with applicable regulatory and operational requirements. For optimization purposes, a Recursive Quadratic Programming method is utilized, while the shafting torsional vibration response is determined using a standard vibration analysis program with slight modifications. Numerical experiments have shown that fast convergence can be achieved. Compared to the classically obtained solution, the proposed approach provided more than 8 % reduction in cost function as well as significantly reduced design time.

Key words: *inertia; optimum design; propulsion shafting; torsional vibration*

1. Introduction

The designs of modern merchant ships tend to maximize the cargo space, which thus reduces space in other parts of the vessel. When looking for space to minimize, the engine room comprising the main engine, auxiliary engines, boilers, and other utilities is the prime candidate. However, there are clear limitations to reducing the engine room space. Firstly, there are physical limitations in terms of placing all equipment into limited smaller sized engine room. Secondly, a limitation is imposed by the minimum length of the propulsion shafting that is needed to retain its torsional vibration stress levels within acceptable limits.

In general, the main engine location is usually selected as the aft-most position allowed by the ships aft body geometry; see, for example [1]. This means the least propeller shaft and intermediate shaft lengths are involved, Fig. 1. The unfavorable consequence of this approach

is the high torsional vibration stress generated on the propulsion shafting [2]. Since modern engines are characterized by maximized combustion pressures and therefore, increased

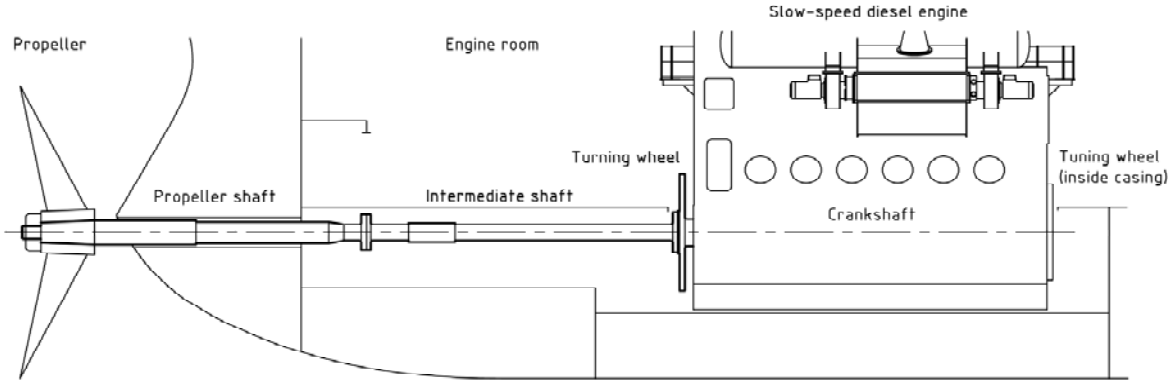

Fig. 1 Typical merchant ship propulsion plant (Note: bearings omitted in order to maintain clarity)

vibration excitations, the correct design of the propulsion shafting design emerges as one of the most challenging tasks during the process of designing the ship's machinery.

The correct design of the marine diesel propulsion shafting was reviewed in the classic work [3], while other important aspects have been covered in greater detailed elsewhere [4-8]. Optimization methods in the design of marine diesel propulsion shafting have mostly been applied in the field of shaft statics [9-11], whereas dynamic responses have rarely been taken into account. All these papers have dealt with the number and optimal positions of the journal bearings, implying the already known shafting, turning wheel, and tuning wheel dimensions. However, no one paper has researched the selection of these dimensions. The optimal selection of shafting dimensions has been the theme of a small poster [12], but no practical realization was provided at that time.

The aim of the present study was to propose a procedure for the selection of the low-speed marine diesel propulsion shafting dimensions, in which the design task is formulated and solved as a constrained nonlinear optimization problem. The proposed procedure takes into account the torsional vibration response of the propulsion plant (because this is the most influential factor that determines the shafting dimensions), an approach which has not hitherto been reported in literature. The applicability of the proposed procedure was examined using a case study of the design of a Suezmax tanker propulsion shafting, which was originally optimized using a classic trial-and-error approach, [2].

The remainder of this paper is organized as follows. In Section 2 the basics of the least inertia design approach are provided. Then, in Section 3, the torsional vibration response of the propulsion shafting is outlined. In Section 4, the specific characteristics of the numerical experiments are reported in more detail. Finally, in Section 5, some conclusions arising from the study are discussed.

2. Least inertia approach

The marine diesel propulsion shafting of a typical merchant ship usually contains the following components: engine crankshaft, intermediate shaft, and propeller shaft, Fig. 1. Regarding the dynamic behavior of the shafting, important additional components include the turning wheel (connected to the crankshaft aft side), tuning wheel (connected to the crankshaft fore side), and the propeller. In cases when a favorable torsional vibration response is able to be obtained, the tuning wheel can be removed from the system. For analysis purposes, the propulsion shafting is usually simplified to a torsional scheme, as shown in Fig. 2.

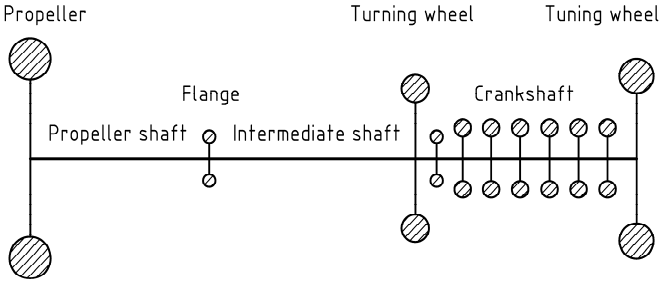

Fig. 2 Torsional vibration scheme of the propulsion system

Shafting inertia and stiffness are the most influential factors that determine the overall torsional vibration behavior of the propulsion system. The constant diameter shaft element inertia, J, and stiffness, k, are defined with:

$$J = \frac{\pi}{32} \cdot \rho \cdot l \cdot d^4 , \tag{1}$$

$$k = \frac{\pi}{32} \cdot \frac{G}{l} \cdot d^4 , \tag{2}$$

where G and ρ are the shaft material shear modulus and density, and l and d are the shaft element length and diameter, respectively. According to Eq. (1) and (2), the lower shaft inertia implies a smaller diameter and lower stiffness. The opposite is also valid.

In general, the smaller shafting inertia systems possess a number of advantages: smaller shaft diameters imply lower material costs in terms of smaller bearings, stern tubes and oil glands, smaller propeller hubs, simplified shaft alignments [13], and reduced propeller-induced variable thrusts [14], that provoke unfavorable engine room and overall ship hull vibrations. However, smaller diameters also imply higher vibration stresses, and thus vibration analyses should be carried out with the utmost care and accuracy. In addition, it should be clearly realized that the inertia of the turning wheel and tuning wheel has a completely opposite influence on the propulsion plant torsional vibration behavior. Specifically, the smaller inertia wheels generally increase the vibration torque, and hence enlarge the vibration stress. Therefore, it is essential to consider the inertia of the whole system, where the shaft inertia and wheel inertias are the constituents. Applied in this way, the least inertia approach ensures a balance between the opposite shaft diameter and wheel size influences.

The rationale behind the least inertia design approach is to select those shafting dimensions, and thus the accompanied components, that minimize the overall inertia of the propulsion system and, at the same time, satisfy all the imposed constraints (e.g. vibration stresses should be within the allowable limits). More formally, the least inertia design approach for the low-speed propulsion shafting system can be defined as follows.

2.1 Design variables

A set of design variables $\mathbf{x} = (x_1, x_2, ..., x_n), \mathbf{x} \in \mathbb{R}^n$, can be assembled in various ways. However, in its simplest form, it can be defined as:

$$\mathbf{x} = \begin{Bmatrix} x_1 \\ x_2 \\ x_3 \\ x_4 \end{Bmatrix} = \begin{Bmatrix} d_{\mathrm{IS}} \\ d_{\mathrm{PS}} \\ J_{\mathrm{FW}} \\ J_{\mathrm{TW}} \end{Bmatrix}, \tag{3}$$

where d_{IS} is the intermediate shaft diameter, d_{PS} is the propeller shaft diameter, J_{FW} is the turning wheel inertia, and J_{TW} is the tuning wheel inertia.

Figure 1 shows that the intermediate shaft and propeller shaft are actually stepped shafts composed of various sections of distinct diameters. However, it can be shown that these stepped shaft diameters are not independent, because they are defined by particular relations [6]. Therefore, with no substantial loss in accuracy, both shafts can be satisfactorily defined by using two unique diameters only, denoted here as d_{IS} and d_{PS}.

More generally, the set of design variables can be expanded by introducing both shaft lengths, the required material properties, and other parameters that define the propulsion plant in greater detail.

2.2 Cost function

The definition of the cost function is a cornerstone of the least inertia propulsion shafting design approach. The cost function is defined as the sum of the inertias of the shafting components. Because some components are predefined, such as the engine crankshaft and propeller, they can be omitted from this definition. In addition, wheel inertias are usually an order of magnitude greater compared with the shafting inertias. Therefore, some kind of inertia scaling is desirable.

Taking these considerations into account, the cost function can be finally set as:

$$f(\mathbf{x}) = w_{\mathrm{S}} \cdot J_S + w_{\mathrm{FW}} \cdot J_{\mathrm{FW}} + w_{\mathrm{TW}} \cdot J_{\mathrm{TW}}, \tag{4}$$

where J_{S} is the shafting inertia, and $w_{\mathrm{S}}, w_{\mathrm{FW}}$, and w_{TW} are the weight factors assigned to the shafting, turning wheel, and tuning wheel inertias, respectively.

It is reasonable to set the weight factor of the shafting inertia equal to unity ($w_{\mathrm{S}} = 1$), and assign smaller values to the other weight factors (values in the range of 0,01 to 0,1 seem to be appropriate). The cost function then implies the corresponding or equivalent shafting inertia. Because the shafting production costs are usually strongly correlated with the shaft dimensions and the sizes of the accompanied equipment, the proposed cost function becomes a suitable proxy of the actual shafting costs.

It is important to realize the true meaning of the selected weight factors. They are not simply pure numbers that scale the contributions of various inertias to the cost function. On the contrary, they are an expression of design intent, namely a designer's will, expressed in a few simple numbers.

Lower weight factors minimize the relative importance of the respective property and thereby allow for higher values of it. By contrast, higher weight factors stress the relative importance of the respective property and thus support its reduction. Further insights into the benefits of these weight factors can be obtained by analyzing the results provided in Section 4.

2.3 Constraints

Constraints are set of conditions that, when met, ensure that design feasibility complies with the pre-agreed classification rules. Furthermore, they help ensure the plant behavior complies with operational requirements. The three mandatory constraints are:

$$g_j(\mathbf{x}) \equiv \frac{\tau_j}{s_j \cdot \tau_{2,j}} - 1 \le 0; \quad j = 1,2,3, \tag{5}$$

where τ_j is the peak vibration stress encountered in the whole engine speed range, $\tau_{2,j}$ is the corresponding stress limit, s_j is the stress limit factor, and j is the index denoting the crankshaft, intermediate shaft, and propeller shaft, respectively. The vibration stress limits, Equation (5), applicable to the crankshaft are defined in [5], or in the enginebuilders documentation, while the corresponding stress limits for the intermediate shaft and propeller shaft are defined in [6].

If more specific requirements are called for, the set of constraints can be easily expanded through additional constraints. Typical candidates are the peak vibration stress limit in the event of irregular firings in one of the engine cylinders, the angular displacement or angular velocity limit of the engine crankshaft, and the position of the so-called barred speed range (Section 4.3).

In addition to these explicit constraints, Eq. (5), a number of implicit constraints can be expressed in the form of variable bounds. For instance, the diameters of both the propeller shaft and the intermediate shaft should be greater or equal to the minimum shaft diameters prescribed by classification bodies, [6]. Furthermore, the dimensions of the turning wheel or tuning wheel should also be within the bounds stipulated or approved by the enginebuilders.

3. Shafting torsional vibration response

The analysis of the torsional vibration response of the propulsion shafting is nowadays a well-developed field that has multiple sources that thoroughly treat its computational aspects [15-18]. The main equation governing the system response is:

$$\mathbf{J}\ddot{\boldsymbol{\varphi}} + \mathbf{C}\dot{\boldsymbol{\varphi}} + \mathbf{K}\boldsymbol{\varphi} = \mathbf{f}\,, \tag{6}$$

where **J** is the inertia matrix, **C** is the damping matrix, **K** is the torsional stiffness matrix, $\boldsymbol{\varphi}$ is the displacement vector, and **f** is the vibration excitation vector.

Equation (6) is a non-homogenous system of linear ordinary differential equations of second order with constant coefficients, which after applying the proper substitution [17], transform into a system of algebraic equations with complex coefficients:

$$-\Omega^2\mathbf{J}\hat{\boldsymbol{\varphi}} + i\Omega\mathbf{C}\hat{\boldsymbol{\varphi}} + \mathbf{K}\hat{\boldsymbol{\varphi}} = \hat{\mathbf{f}}\,, \tag{7}$$

where Ω is the excitation frequency, i is the imaginary unit, and $\hat{\boldsymbol{\varphi}}$ and $\hat{\mathbf{f}}$ are the vectors of the complex angular displacement and excitation amplitudes, respectively. The number of equations in Eq. (7) corresponds to the number of lumped masses in the torsional vibration scheme, Fig. 2.

Vibration analysis starts by calculating the natural vibration (eigenvalue problem), [17], where the plant's natural frequencies, mode shapes, and critical speeds are determined. Then, a forced vibration response is calculated, including working out the angular displacements of all system masses. After that, the remaining process is straightforward: the vibration torques are calculated using the shaft stiffness properties and finally the vibration stresses are determined.

This analysis process refers to one harmonic of the vibration excitation. Because the actual vibration excitation is of the periodic form, a series of responses should be calculated and synthesized until the total response is obtained. In addition, the whole process should be repeated multiple times for various engine speeds within the operating speed range.

4. A *Suezmax* tanker case study

The proposed approach was used during the development of a *ShaftOpt v1.0* design tool that provides the optimum dimensions of a propulsion shafting in terms of its torsional vibration behavior. The case study of a 166300 dwt Suezmax oil tanker is used to demonstrate the utility of this program.

The basic design data are provided in Tables 1 and 2. Other engine-specific data can be obtained from the enginebuilders documentation.

4.1 Optimization problem

The studied tanker [19] is characterized by a relatively small engine room (22,95m in length), with the engine located in the foremost position given the limited engine room space available, Fig. 1.

The design of the propulsion shafting can be defined as an optimization problem where the vector of the design variables, Eq. (3), should be determined to minimize the cost function, Eq. (4), such that a set of constraint functions, Eq. (5), is satisfied.

4.2 Optimization method

For optimization purposes, we use a variant of the Recursive Quadratic Programing method (RQP; also known as Sequential Quadratic Programing, SQP), [20]. This method was originally developed by Pshenichny [21], and further improved by Lim and Arora [22], and Belegundu and Arora [23]. The method possesses a number of favorable properties, including a sound theoretical foundation, proof of global convergence with a potential constraint strategy, and a good track record of reliability and efficiency [24].

Pshenichny's method minimizes a descent function:

$$F(\mathbf{x}) = f(\mathbf{x}) + r \cdot V(\mathbf{x}), \tag{8}$$

Table 1 Main engine particulars

Diesel engine type	2-stroke	
Rated power	16780	kW
Rated speed	82	rpm
Minimum speed	20	rpm
Number of cylinders	6	
Cylinder bore	700	mm
Piston stroke	2800	mm
Mean indicated pressure	20	bar

Table 2 Propulsion shafting data

Propeller inertia	141500	kgm^2
Propeller shaft length	8430	mm
Propeller shaft material UTS[a)]	600	N/mm^2
Intermediate shaft length	8000	mm
Intermediate shaft material UTS[a)]	600	N/mm^2

[a)] Ultimate Tensile Strength

where r is the penalty parameter, and $V(\mathbf{x})$ is the maximum constraint violation, defined by:

$$V(\mathbf{x}) = \max \begin{pmatrix} 0, \\ \left| g_j(\mathbf{x}) \right|, \ j = 1 \text{ to } m' \\ g_j(\mathbf{x}), \ j = m'+1 \text{ to } m \end{pmatrix}, \tag{9}$$

where m' is the number of equality constraints, m is the total number of constraints, and inequality constraints are of the $g_j \le 0$ form. Since all constraints, Eq. (5), are normalized [25], the maximum constraint violation $V(\mathbf{x})$ suggests the maximum percentage stress limit violation (e.g. $V(\mathbf{x})$ = 0,485 means that the peak vibration stress is 48,5% higher than the corresponding stress limit). At the optimum, the cost function is equal to the descent function value, since the constraint violation for the feasible point should be equal to zero.

The optimization algorithm is coded in *RQPOpt v2.3* general purpose optimization software. This algorithm utilizes a specific active set strategy that employs only a fraction of the overall total of constraints during the search direction subproblem. In addition, a significant feature of the software is an interactive recovery routine that enables further progress in cases when no improvement is achieved within the predefined number of line search attempts. This routine offers three modes of numerical recovery [25]. The first one is a reset of the Hessian matrix of the Lagrangian function, when the Hessian matrix is set to unity. The second one is an expansion of the active constraint set, when all constraints are included in the set during the search direction subproblem. Finally, the third mode reduces the constraint violation irrespective of the possible rise in the cost function.

4.3 Optimization runs

In order to better understand the influence of the weight factors related to the cost function, Eq. (4), it was decided to perform a series of optimization runs, each with different weights prescribed and/or different starting points.

Table 3 comprises 12 series of the weight factors that were applied to the cost function. In all trials, the shafting weight factor was set to unity, while the weight factors for the tuning wheel and the turning wheel were varied. Table 3 has four weight factor blocks, each containing three options. The first one gives equal weight to both wheels, whereas the second and third options give preference to reducing the tuning wheel or the turning wheel, respectively. The relative difference between the two weights and the basic one is set to ±20%.

Since the optimization problem is not unimodal (at least two local minima are expected), for each combination of weight factors three starting points were adopted (Table 4), thereby raising the total number of optimization runs to 36.

The *Mini* starting point (Table 4) resembles the minimum dimensions stipulated by the classification bodies [6], or allowed by the enginebuilders. This starting point is deeply infeasible, as the maximum constraint violation of 0,485 indicates, Fig.3. In addition to the stress response of the shafting vibration, this figure includes two curves that represent the stress limits imposed. The lower one (denoted by τ_1) represents the stress limit for the continuous running of the engine, whereas the upper one (denoted by τ_2) represents the stress limit for the transient running of the engine. The τ_1 stress limit can be violated for a limited time only, whereas τ_2 should not be violated under any circumstances. The engine speed

Table 3 Cost function weight factors

Series	w_{TW}	w_{FW}	w_S
A	0,01	0,01	1,0
B	0,012	0,008	1,0
C	0,008	0,012	1,0
D	0,02	0,02	1,0
E	0,024	0,016	1,0
F	0,016	0,024	1,0
G	0,05	0,05	1,0
H	0,06	0,04	1,0
I	0,04	0,06	1,0
J	0,1	0,1	1,0
K	0,12	0,08	1,0
L	0,08	0,12	1,0

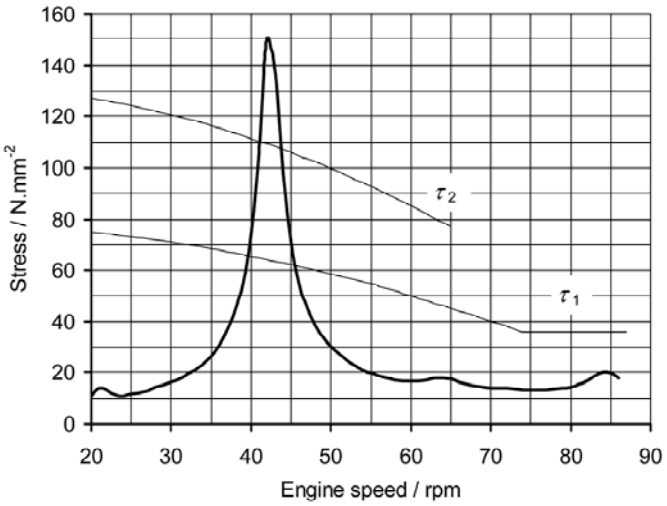

Fig. 3 Intermediate shaft stress response for the first starting point

range where the actual vibration stress exceeds τ_1 stress limit is referenced as the barred speed range.

The *Maxi* starting point (Table 4), by contrast, includes the maximum turning wheel and tuning wheel allowed by the enginebuilders. The maximum starting diameters of the propeller shaft and intermediate shaft are selected as 20% higher values compared with the corresponding minimum one. This starting point is feasible, as indicated by $V(\mathbf{x})=0$, Table 4.

Finally, the *Midi* starting point (Table 4) is assembled of values that are in the middle of the previous two. The corresponding maximum constraint violation is equal to 0,106, indicating the moderate infeasibility.

During the evaluation of the constraints, Equation (5), the following stress limit factors are used: $s_1 = 0{,}95$ and $s_2 = s_3 = 0{,}92$. These values provide a safety margin for cases when the peak vibration stresses are additionally elevated owing to irregular firings in some of the engine cylinders.

In order to calculate the torsional vibration response, a *TorViC* [26] computer code is used, although the basic code is slightly modified to enable analysis calls by the optimization package. At the source-code level, the analysis program is transformed into the subroutine and the subroutine arguments are used to communicate between the optimization and analysis programs. All analysis program outputs are suppressed. The ordinary analysis includes a vast number of evaluations of the forced vibration response within the whole engine speed range. For optimization purposes only, a subset of these response evaluations is carried out, depending on the resonances determined in the natural vibration analysis phase.

Table 4 Starting points

Point	Mark	d_{IS}	d_{PS}	J_{FW}	J_{TW}	$V(\mathbf{x})$
1	Mini	532	650	13150	0	0,485
2	Midi	580	720	27000	30000	0,106
3	Maxi	640	780	42000	60000	0,0

The specific RQP optimization algorithm parameters used [20] are summarized in Table 5.

Table 5 Optimization algorithm parameters

Pshenichny's constraint set constant	δ_0	0,1
Penalty parameter	r_0	1,0
Stopping tolerance	ε_d	$1,0\times10^{-5}$
Constraint violation tolerance	ε_{cv}	$1,0\times10^{-3}$
Finite difference parameter	Δ	$1,0\times10^{-5}$

All programs were compiled using a Compaq Visual Fortran 6.6C compiler and carried out on a standard PC workstation equipped with a 2,13 GHz dual-core processor, 2 GB RAM, and the MS Windows XP Professional SP3 operating system.

4.4 Results

All 36 optimization runs completed successfully. However, this was not a straightforward process, because a significant number of runs experienced numerical difficulties because of failure to find a better point during the line search process. Hence, the program's interactive recovery capability was extensively used and the active constraint set expansion was utilized in most cases. However, irrespective of whichever recovery measures were applied, some optimization runs still finished owing to their inability to progress any further. Hopefully, all these runs finished within the feasible region.

The mid-range approximation feature [20] was not used during the line search process because this frequently requires an increased number of iterations. However, variable scaling [27] proved favorable in that a significant degree of efficiency improvement was achieved. This was expected because the design variables differed in size by nearly two orders of magnitude. A typical convergence history is shown in Figure 4.

The results of each cost function weight factor group (Table 3) were then compared and the best-run results are shown in Table 6 (the letters denote the weight factors group, and the numbers entail the starting point). Assembled this way, Table 6 represents a collection of the optimum results achieved by using various cost function weight factors.

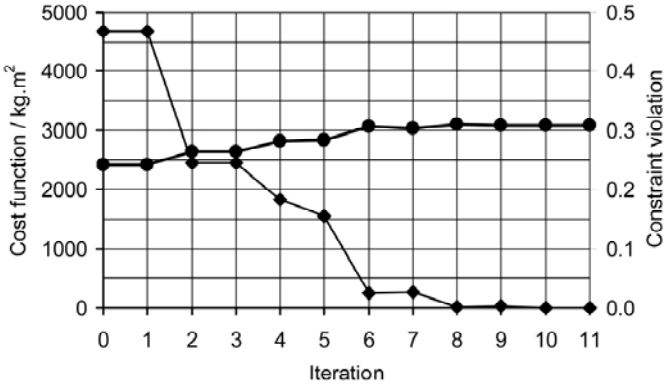

Fig. 4 Convergence history for the B-1 case

Table 6 Optimum results achieved

Case	d_{IS}	d_{PS}	J_{FW}	J_{TW}	$f(\mathbf{x}*)^{a)}$	$V(\mathbf{x}*)$	NIT	NFE	NGE	CPUT
A–3	536,7	650	13150	57487	3010,0	0,0	6	45	67	38,942
B–1	542,8	650	42000	34161	3084,0	$1,8\times10^{-5}$	11	75	133	66,956
C–2	533,2	650	13150	59172	2915,5	$1,3\times10^{-4}$	5	42	70	36,002
D–2	578,0	650	13150	40405	3629,7	0,0	8	73	125	66,432
E–1	587,3	650	42000	17129	3705,5	0,0	11	76	148	62,366
F–2	568,9	650	13150	43765	3514,3	0,0	9	75	125	67,006
G–2	588,4	650	13150	36793	5127,4	0,0	9	46	90	48,654
H–1	587,3	650	42000	17129	5330,1	0,0	11	76	154	66,703
I–3	584,4	650	13150	38162	4917,7	0,0	13	100	169	91,581
J–3	584,4	650	13150	36793	7624,5	0,0	12	73	119	69,878
K–3	584,4	650	42000	16762	8001,7	0,0	12	73	119	57,975
L–3	584,4	650	13150	36793	7151,7	0,0	12	62	104	54,332

[a)]Cost functions are not mutually comparable because of the use of different weight factors
NIT – Number of iterations, NFE – Number of cost function evaluations,
NGE – Number of constraint function evaluations (each constraint counted separately),
CPUT – Execution time in seconds, $\mathbf{x}*$ – optimum design vector

It is worth noting that these cost function values should not be claimed as an advantage during the comparison of the optimal solutions provided in Table 6. This is because each table entry refers to different definitions of the cost function and thereby represents a solution to different optimization problems. Therefore, an engineering judgment is more appropriate.

At first sight, each set of results in Table 6 seem different. However, when analyzed in more detail, these results become more transparent and point to two principal outcomes only, depending on the size of the turning wheel.

The first principal solution is based on the minimum turning wheel (J_{FW} = 13150 kgm^2), whereas the second one utilizes the maximum turning wheel that is available (J_{FW} = 42000 kgm^2). It is interesting to note that in both cases, the propeller shaft diameter is minimal (d_{PS} = 650 mm). The remaining design variable values (tuning wheel inertia and intermediate shaft diameter) strongly depend on the cost function weight factors applied.

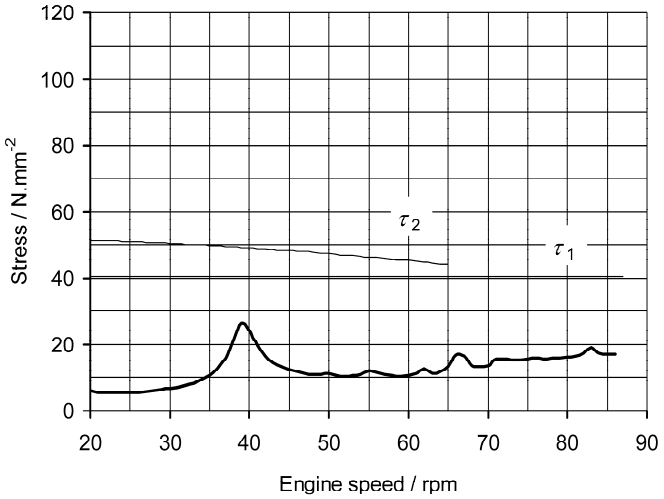

Fig. 5 Crankshaft stress response for the C–2 case

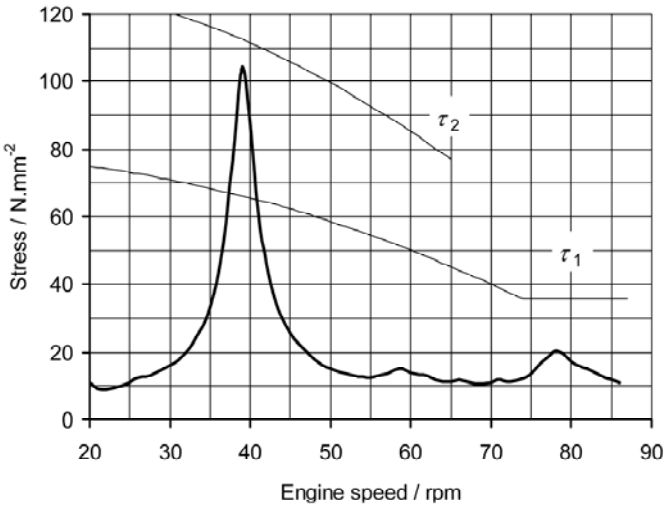

Fig. 6 Intermediate shaft stress response for the C–2 case

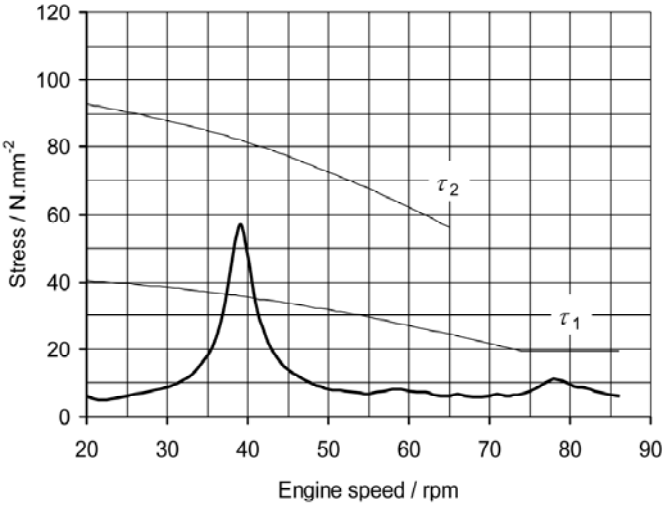

Fig. 7 Propeller shaft stress response for the C–2 case

If a small turning wheel is preferred, the solution denoted by C–2 is the best choice (d_{IS} = 533,2 mm, and J_{TW} = 59172 kgm^2), because this minimizes the shafting as well as the

accompanied equipment costs (e.g. bearings, sterntube, and propeller hub). Figures 5, 6, and 7 shows the corresponding torsional vibration responses for the crankshaft, intermediate shaft and propeller shaft, respectively.

If, however, a large turning wheel is selected, the solution denoted by B–1 is the next most favorable candidate (d_{IS} = 542,8 mm, and J_{TW} = 34161 kgm^2).

Table 6 also provides other possibilities that may become interesting depending on a shaft diameter and wheel size preferences.

It is interesting to compare these results with the result derived in the real project environment that was obtained using a simple *trial-and-error* approach [2]. After more than two dozen design iterations that took a full month to complete, the final results were d_{IS} = 585 mm, d_{PS} = 650 mm, J_{FW} = 13150 kgm^2, and J_{TW} = 45000 kgm^2. When compared with the J–3 and L–3 results (the most similar results shown in Table 6), the corresponding cost functions become $f(\mathbf{x}^*)$ = 8421,6 kgm^2 and $f(\mathbf{x}^*)$ = 7784,6 kgm^2, respectively, depending on the weight factors used. Compared with the classically obtained solution, the proposed approach provided a more than 8% reduction in cost function as well as significantly reduced development time.

5. Conclusions

The proposed procedure is based on the shafting least inertia principle, when shafting dimensions are used that minimize the inertia of the propulsion plant while fulfilling the torsional vibration stress constraints.

The benefits of the proposed approach are threefold. First, it can efficiently determine feasible designs that fully comply to classification society rules and other design requirements. Second, it provides design solutions that have a series of favorable features such as lower material and production costs, a simplified shaft alignment, and reduced propeller-induced variable trust remedies. Finally, by varying the cost function weight factors, it can generate different optimal solutions depending on the designer's preferences.

Numerical experiments have shown that fast convergence of the resulting nonlinear optimization task can be achieved. They have also shown that the proposed procedure provides cost-effective designs and reduces design time.

Acknowledgement

This work has been partly supported by the Ministry of Science, Education, and Sports through the Project 023-0231744-1745 and the CADEA company.

REFERENCES

[1] Ploeg, A. V. D.: "A comparison of several strategies to optimize a ship's aft body", Journal of Ship Production and Design, 27(2011), 202-211.

[2] MAGAZINOVIĆ, G.: "Significance of shafting length - A Suezmax tanker design problem", Proceedings, Paper No. 40, IMAM 2002 Congress, Rethimno 2002.

[3] LONG, C. L.: "Propellers, shafting, and shafting system vibration analysis", in: R. L. Harrington (Ed.), Marine Engineering, The Society of Naval Architects and Marine Engineers, Jersey City, 1992, 353-411.

[4] DAHLER, G., ROALDSØY, J., SANDBERG, E.: "Det Norske Veritas' methodology for propulsion shaft design - A cost-saving and reliable supplement to the IACS simplified code", Proceedings, SNAME Symposium on Propellers/Shafting, Williamsburg 1992.

[5] "Calculation of crankshafts for I.C. engines", M53, International Association of Classification Societies, London 2011.

[6] "Dimensions of propulsion shafts and their permissible torsional vibration stresses", M68, International Association of Classification Societies, London 2012.

[7] SCHIFFER, W.: "Advanced methods for static and dynamic shafting calculations", Brodogradnja, 58(2007)2, 158-164.

[8] "Calculation of shafts in marine applications", Classification Notes No. 41.4, Det Norske Veritas, Høvik 2007.

[9] BRADSHAW, R. T.: "The optimum alignment of marine shafting", Marine Technology, 11(1974)3, 260-269.

[10] MOURELATOS, Z., PAPALAMBROS, P.: "A mathematical model for optimal strength and alignment of a marine shafting system", Journal of Ship Research, 29(1985)3, 212-222.

[11] ŠVERKO, D.: "Shaft alignment optimization", Proceedings, 17th Symposium on Theory and Practice of Shipbuilding, Opatija 2006.

[12] MAGAZINOVIĆ, G.: "Optimization as a marine propulsion shafting system design tool", Proceedings, 10th International Conference on Engineering Design - ICED'95, Prague 1995.

[13] ŠVERKO, D.: "Design concerns in propulsion shafting alignment", ABS Technical Papers, Houston 2003.

[14] BRYNDUM, L., JAKOBSEN, S. B.: "Vibration characteristics of two-stroke low speed diesel engines", Proceedings, 9th International Marine Propulsion Conference, London 1987.

[15] HAFNER, K. E., MAASS, H.: "Theorie der Triebwerksschwingungen der Verbrennungskraftmaschine", Springer Verlag, Wien 1984.

[16] HAFNER, K. E., MAASS, H.: "Torsionsschwingungen in der Verbrennungskraftmaschine", Springer Verlag, Wien 1985.

[17] WALKER, D. N.: "Torsional Vibration of Turbomachinery", McGraw-Hill, New York 2004.

[18] FRISWELL, M. I., PENNY, J. E. T., GARVEY, S. D., LEES, A. W.: "Dynamics of Rotating Machines", Cambridge University Press, Cambridge 2010.

[19] ČUDINA, P.: "Research & development Supercargo project (II)", Brodogradnja, 49(2001), 55-60.

[20] MAGAZINOVIĆ, G.: "Two-point mid-range approximation enhanced recursive quadratic programming method", Structural and Multidisciplinary Optimization, 29(2005), 398-405.

[21] PSHENICHNY, B. N.: "The Linearization Method for Constrained Optimization", Springer Verlag, Haidelberg 1996.

[22] LIM, O. K., ARORA, J. S.: "An active set RQP algorithm for engineering design optimization", Computer Methods in Applied Mechanics and Engineering, 57(1986), 51-65.

[23] BELEGUNDU, A. D., ARORA, J. S.: "A recursive quadratic programming method with active set strategy for optimal design", International Journal for Numerical Methods in Engineering, 20(1984), 803-816.

[24] PATNAIK, S. N., CORONEOS, R. M., GUPTILL, J. D., HOPKINS, D. A.: "Comparative evaluation of different optimization algorithms for structural design applications", International Journal for Numerical Methods in Engineering, 39(1996), 1761-1774.

[25] ARORA, J.: "Introduction to Optimum Design", McGraw-Hill, New York 1989.

[26] MAGAZINOVIĆ, G.: "*TorViC v1.1* – Program for Propulsion System Torsional Vibration Analysis", User's Guide, CADEA, Split 2000 (in Croatian).

[27] MAGAZINOVIĆ, G.: "Scaling of variables - An efficient way of design optimization process improvement", Proceedings, 5th International Design Conference - DESIGN'98, Dubrovnik 1998.

Submitted: 02.07.2014

Accepted: 09.09.2014

Gojko Magazinović
Faculty of Electrical Engineering, Mechanical Engineering and Naval Architecture
R. Boškovića 32, 21000 Split, Croatia
E-mail: gmag@fesb.hr